

### 5.3. Amundsen-Scott South Pole Station (1/17/06–1/24/07)

The 2006–2007 season at Amundsen-Scott South Pole Station is defined as the period between the site visit on 1/15/06–1/18/06 and system inspection on 1/24/07–1/25/07. Season opening and closing calibrations were performed during the periods 1/17/06–1/18/06 and 1/24/07–1/25/07, respectively. Volume 16 solar data comprise the period 1/17/06–1/24/07. A total of 17690 scans are part of the published South Pole Volume 16 dataset. About 4% of all possible scans are missing because of technical problems, including station-wide power outages.

The SUV-100 spectroradiometer performed well during the reporting period. However, comparisons between measured spectra and results from a radiative transfer model indicated that the cosine error of the SUV-100 had changed during the period of winter darkness. It is possible that the change occurred when the instrument's detector was removed at the beginning of September for cleaning its underside. The change of the cosine error was corrected during processing of Version 2 data, but has not been addressed for Version 0 data described in this report.

The sensitivity of the 320 nm channel of the GUV-541 radiometer changed by 6.5% over the course of the year. GUV data was segregated into two periods and different calibration factors were applied for each period. Drifts in published GUV data are smaller than 3%.

#### 5.3.1. Irradiance Calibration

The site irradiance standards for the 2006/07 season were the lamps 200W021, 200W006, and M-666. Lamp 200W017 was used as traveling standard. This lamp was calibrated by Optronic Laboratories in March 2001.

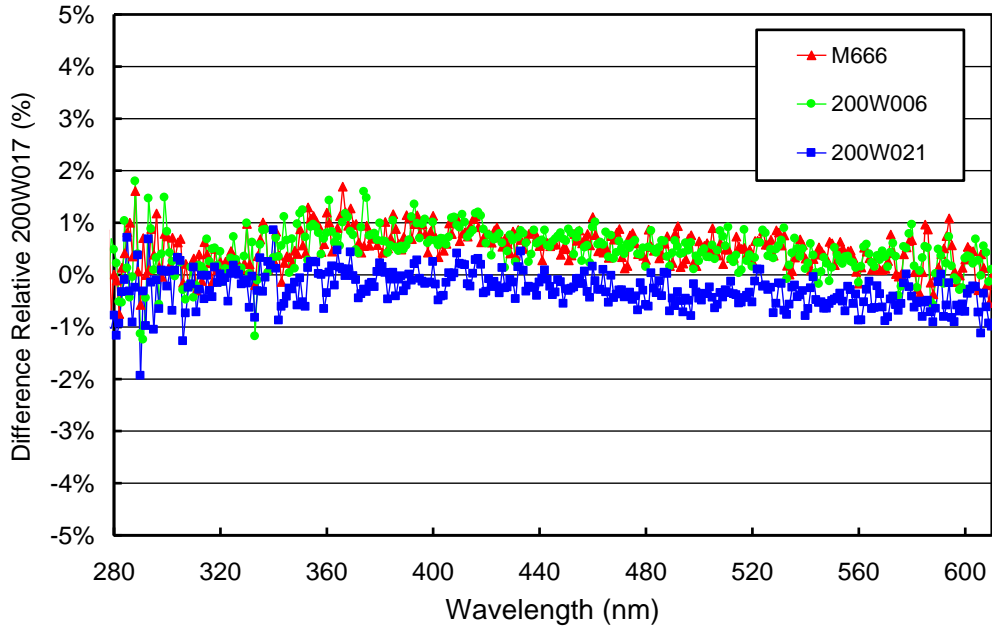
The original calibration of lamp 200W021 was established by Optronic Laboratories in September 1998. Lamp M-666 was originally calibrated with lamps 200W006 and 200W021, using season closing scans of Volume 9 and opening scans of Volume 10.

Based on comparisons performed during the site visit in January 2006, it was determined that lamps 200W021 and M-666 had drifted by about 2%. New calibration were transferred to the lamp using the traveling standard 200W017 as reference, and these calibrations were used to process solar data from the 2006/07 season. Details of the calibration transfer are provided in the Volume 15 Operations Report.

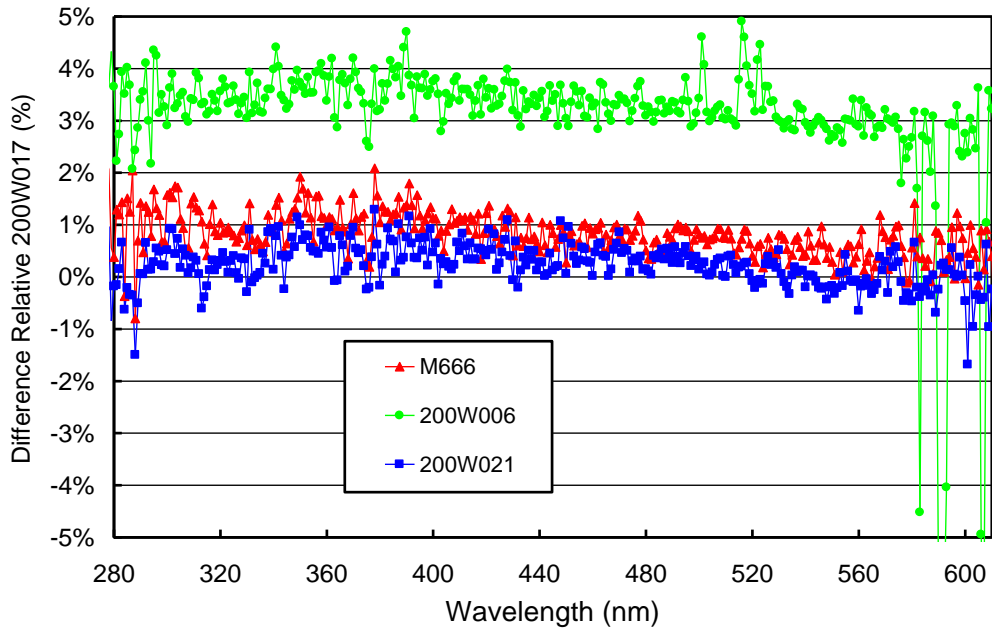
Lamp 200W006 was originally calibrated by Optronic Laboratories in November 1996. The lamp was dropped during the site visit in 2004 and recalibrated against M-764 using data measured on 1/28/04. The lamp proved to be stable during the 2004/05 and 2005/06 seasons despite the mechanical stress that it had suffered. The lamp became unstable in December 2006 and was used for calibration of the SUV-100 spectroradiometer only until 11/4/06.

Figure 5.3.1 shows a comparison of lamps 200W006, 200W021, and M-666 with traveling standard 200W017 at the start of the season (1/17/06–1/18/06). The figure indicates that the calibration of all site standards agreed with the traveling standard to within  $\pm 1\%$ . Figure 5.3.2 shows a similar comparison at the end of the season (1/24/07–1/25/07). Lamps 200W021 and M-666 agreed with lamp 200W017 at the same level as one year earlier. The calibration of lamp 200W006 was different by 3.5% and exhibited instabilities for wavelengths above 500 nm, confirming the lamp's demise.

The three site standards were also compared with each other on 3/26/06 and 9/9/06. The lamps' calibrations agreed to within  $\pm 1\%$  on both occasions.



**Figure 5.3.1.** Comparison of South Pole lamps 200W006, 200W021, and M-666 with BSI traveling standard 200W017 at the start of the season (1/17/06–1/18/06).



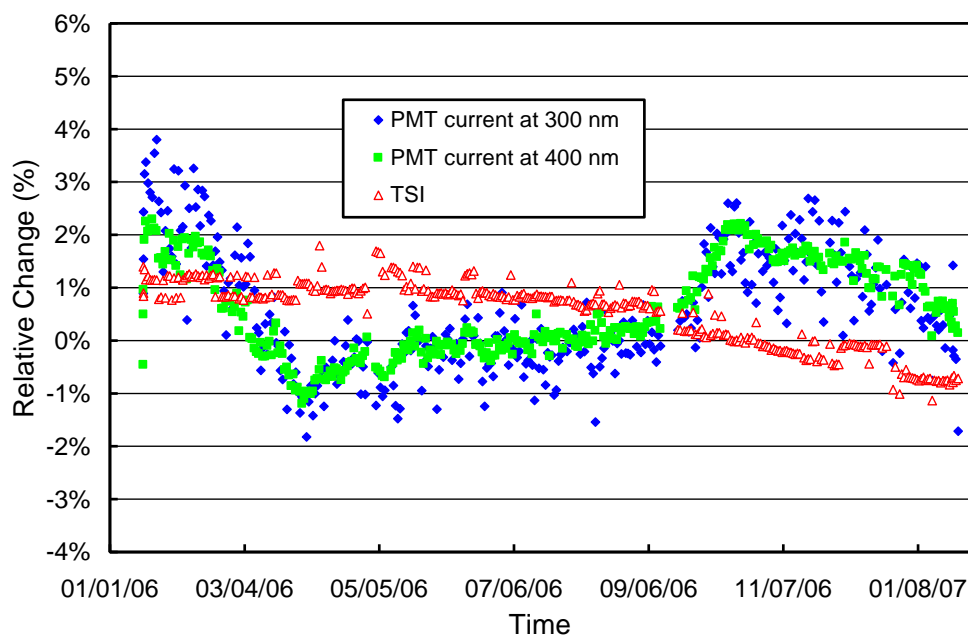
**Figure 5.3.2.** Comparison of South Pole lamps 200W006, 200W021, and M-666 with BSI traveling standard 200W017 at the end of the season (1/24/07–1/25/07).

### 5.3.2. Instrument Stability

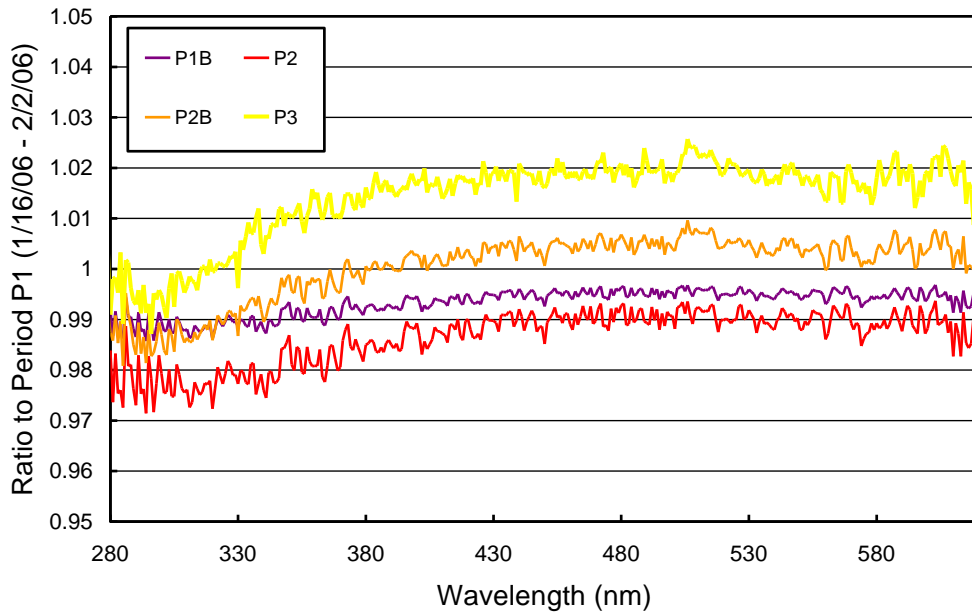
The stability of the spectroradiometer over time is primarily monitored with bi-weekly calibrations utilizing site irradiance standards, and daily response scans of the internal irradiance reference lamp. The stability of the internal lamp is monitored with the TSI sensor, which is independent from possible monochromator and PMT drifts.

Figure 5.3.3 shows changes in TSI readings and PMT currents at 300 and 400 nm, derived from the daily scans of the internal lamp during the South Pole 2006/07 season. The TSI measurements indicate that the internal lamp became dimmer by about 2% during this period. This amount of drift is typical. The PMT currents at 300 and 400 nm varied by less than  $\pm 2\%$ , indicating good stability of the instrument.

Absolute calibrations indicated some variation of the system responsivity related to transmission changes of the irradiance collector, most likely caused by ice-buildup underneath the cosine diffuser. To correct for these changes, 11 different calibration functions were applied to the solar measurements of Volume 16. Calibrated data were compared with measurements of the collocated GUV-541 radiometer. An overview of the calibration periods is provided in Table 5.3.1. Figure 5.3.4 shows ratios of the calibration functions applied between the start of the Volume 16 period and the onset of Polar Night (Periods P1 – P3). Calibrations were consistent to within  $\pm 2.5\%$ . Figure 5.3.5 shows ratios of the calibration functions applied between the end of Polar Night and January 2007 (Periods P5 – P8). Calibrations were consistent to within  $\pm 5\%$ . The increased variability for the second part of the year was likely caused by sublimation and thawing of ice underneath the instrument's collector. Noticeable ice build-up was found on 9/1/06 when the collector was inspected and cleaned. Comparisons with results of a radiative transfer model indicated that the instrument's cosine error may have changed when the collector was removed for inspection. This change was corrected during the processing of Version 2 data and is not further discussed here.



**Figure 5.3.3.** Time-series of PMT current at 300 and 400 nm, and TSI signal for measurements of the internal irradiance standard performed during the South Pole 2006/07 season. Data are normalized to the average of the whole period.



**Figure 5.3.4.** Ratios of irradiance assigned to the internal lamp before Polar Night, relative to Period P1.

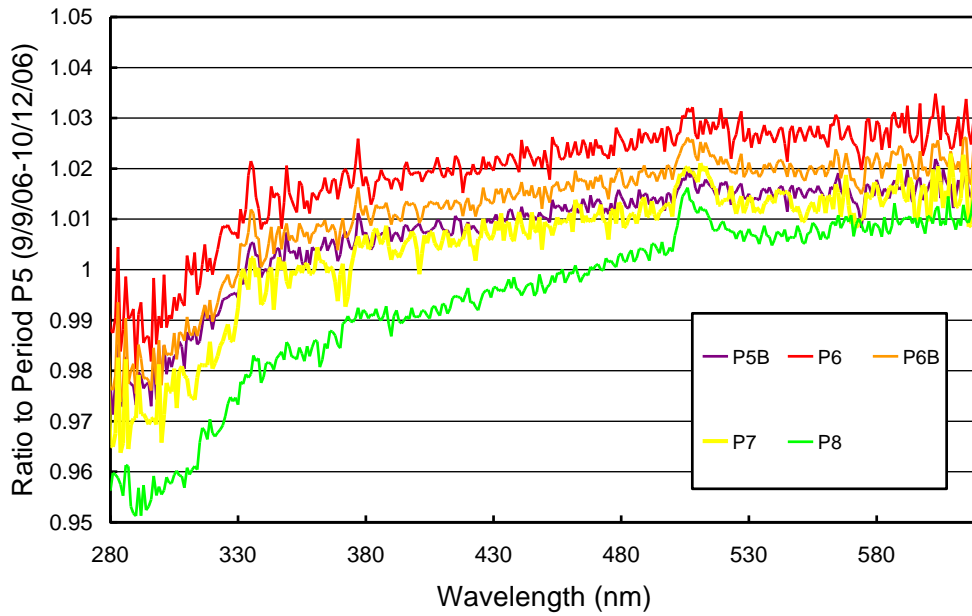


**Figure 5.3.5.** Ratios of irradiance assigned to the internal lamp after Polar Night, relative to Period P5.

Figure 5.3.6 presents the relative standard deviation calculated from the individual calibration scans of each period. These data are useful for estimating the variability of calibrations in each period. The variability is typically less than 1% for wavelengths above 300 nm, indicating very good stability for all periods.

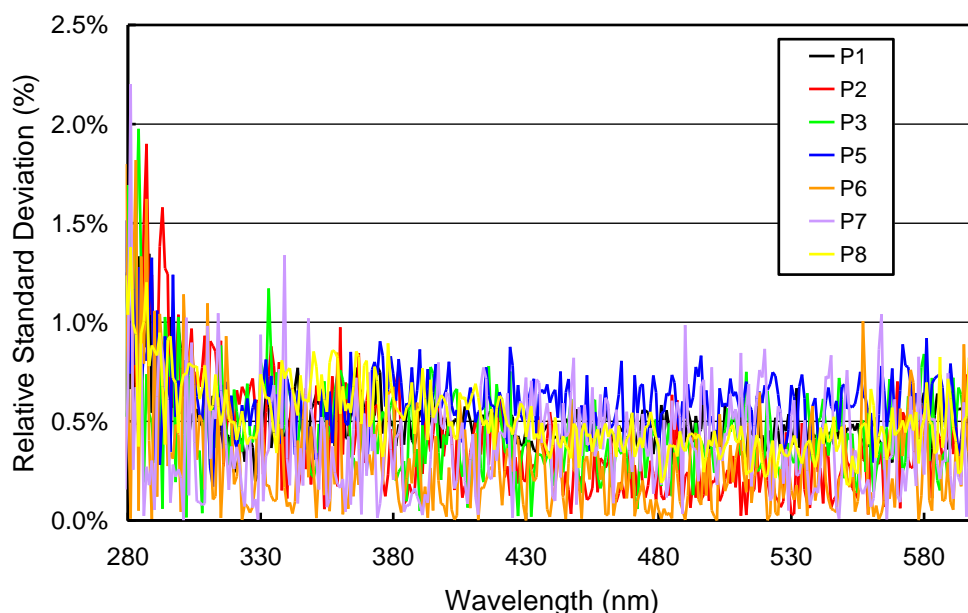


**Figure 5.3.6.** Relative standard deviation calculated from the absolute calibration scans measured during the South Pole 2006/07 season.

**Table 5.3.1: Calibration periods for South Pole Volume 16 data.**

Period name	Period range	Number of Absolute Scans	Remarks
P1	01/16/06 – 02/02/06	10	
P1B	02/03/06 – 02/07/06	0	Interpolated from Periods P1 and P2
P2	02/08/06 – 03/14/06	3	
P2B	03/15/06 – 03/21/06	0	Interpolated from Periods P2 and P3
P3	03/22/06 – 06/21/06	3	Last period before Polar Night
P5	06/22/06 – 10/12/06	5	First period after Polar Night
P5B	10/13/06 – 10/17/06	0	Interpolated from Periods P5 and P6
P6	10/18/06 – 11/08/06	2	
P6B	11/09/06 – 11/14/06	0	Interpolated from Periods P6 and P7
P7	11/15/06 – 12/25/06	2	
P8	12/26/06 – 01/26/07	8	

### 5.3.3. Wavelength Calibration

Wavelength stability of the system was monitored with the internal mercury lamp. Information from the daily wavelength scans was used to homogenize the data set by correcting day-to-day fluctuations in the wavelength offset. After this step, there may still be a deviation from the correct wavelength scale, but this bias should be similar for all days. Figure 5.3.7 shows the difference of the wavelength offset of the 296.73 nm mercury line between two consecutive wavelength scans. In total, 416 scans were evaluated. The change in offset was smaller than  $\pm 0.025$  nm for 91% of the scans and smaller than  $\pm 0.055$  nm for 97% of the scans. The shifts of 11 scan-pairs was larger than  $\pm 0.1$  nm and were caused by operator intervention following power outages. The wavelength calibration was adjusted accordingly.

After data were corrected for day-to-day wavelength fluctuations, the wavelength-dependent bias between this homogenized data set and the correct wavelength scale was determined with the Version 2 Fraunhofer-line correlation method (Bernhard *et al.*, 2004). The resulting correction function is shown in Figure 5.3.8. Corrections exceed 1 nm for wavelengths larger than 500 nm. The magnitude of the correction is considerably larger than for other sites and is caused by the properties of the monochromator installed. The accuracy of solar data is not compromised, since the correction is well defined.

After data had been wavelength corrected using the shift-function described above, the wavelength accuracy was tested again with the Version 2 Fraunhofer-line correlation method. The results are shown in Figure 5.3.9 for four UV wavelengths. The standard deviation of the residual shifts is 0.03 nm. The actual wavelength uncertainty of the instrument may be slightly larger as indicated in Figure 5.3.8 due to wavelength fluctuations during a given day (Figure 5.3.8 shows only one point per day), and possible systematic errors of the Fraunhofer-correlation method (Bernhard *et al.*, 2004).

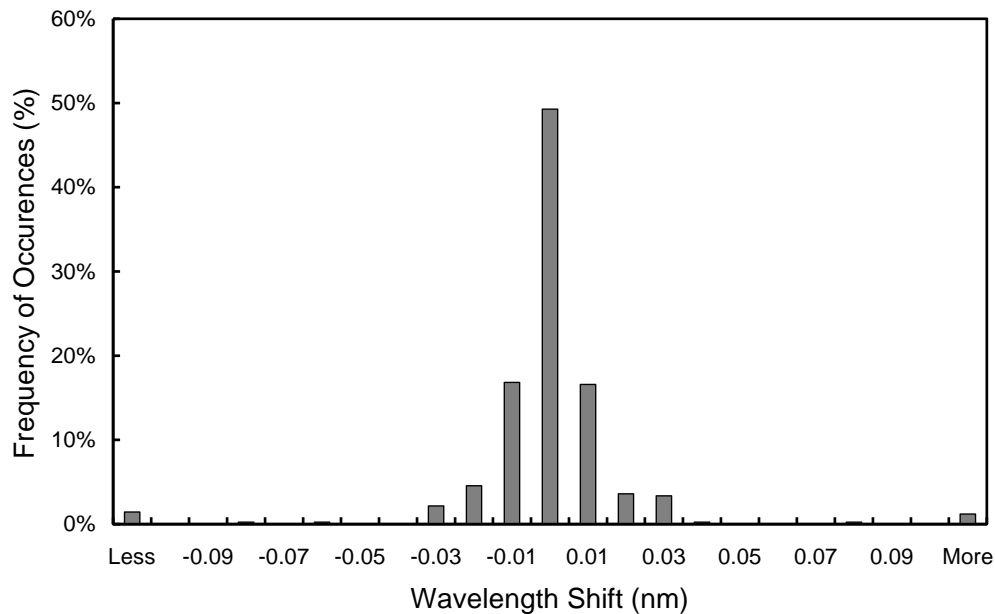


**Figure 5.3.7.** Frequency distribution of the difference of the measured position of the 296.73 nm mercury line between consecutive wavelength scans. The x-labels give the center wavelength shift for each column. The 0-nm histogram column covers the range  $-0.005$  to  $+0.005$  nm. “Less” means shifts beyond  $-0.105$  nm; “more” means shifts beyond  $+0.105$  nm.

Data from the external mercury scans do not have a direct influence on data products but are an important part of instrument characterization. Figure 5.3.10 illustrates the difference between internal and external mercury scans collected during the 2006 and 2007. Measurements of the two years are consistent. The wavelength scale of the figure is the same as applied during solar measurements. The peak of the external scans agrees well with the nominal wavelength of 296.73 nm, whereas the peak of the internal scans is shifted about 0.10 nm to shorter wavelengths. External scans have a bandwidth of about 1.04 nm FWHM. The bandwidth of the internal scan is 0.73 nm. External scans have the same light path as solar measurements and therefore represent the monochromator’s bandpass at 297 nm that is relevant for solar scans.

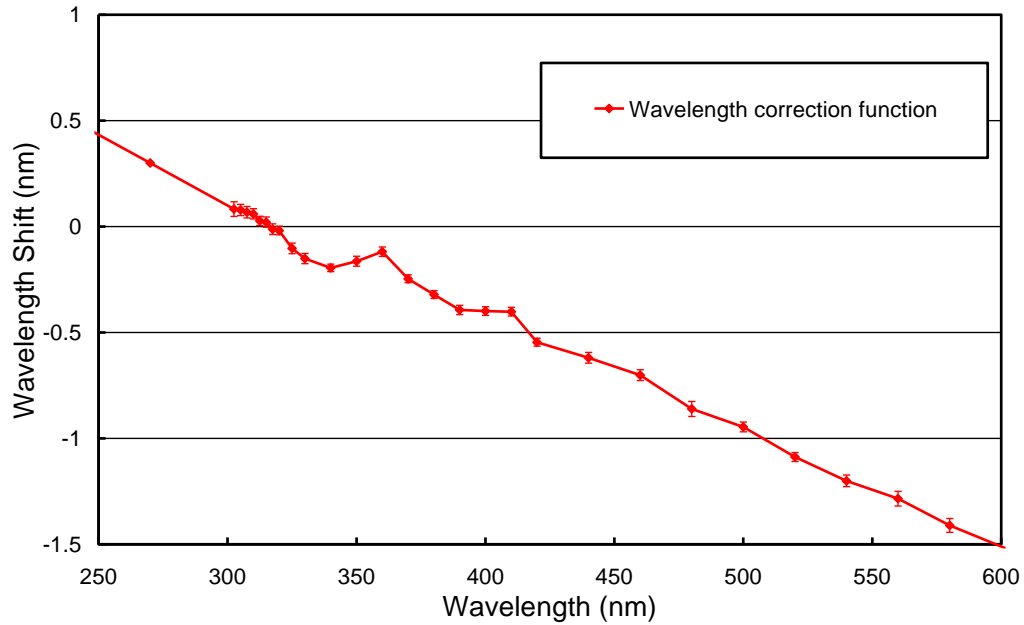


**Figure 5.3.8.** Monochromator non-linearity correction function for the South Pole 2006/07 season.

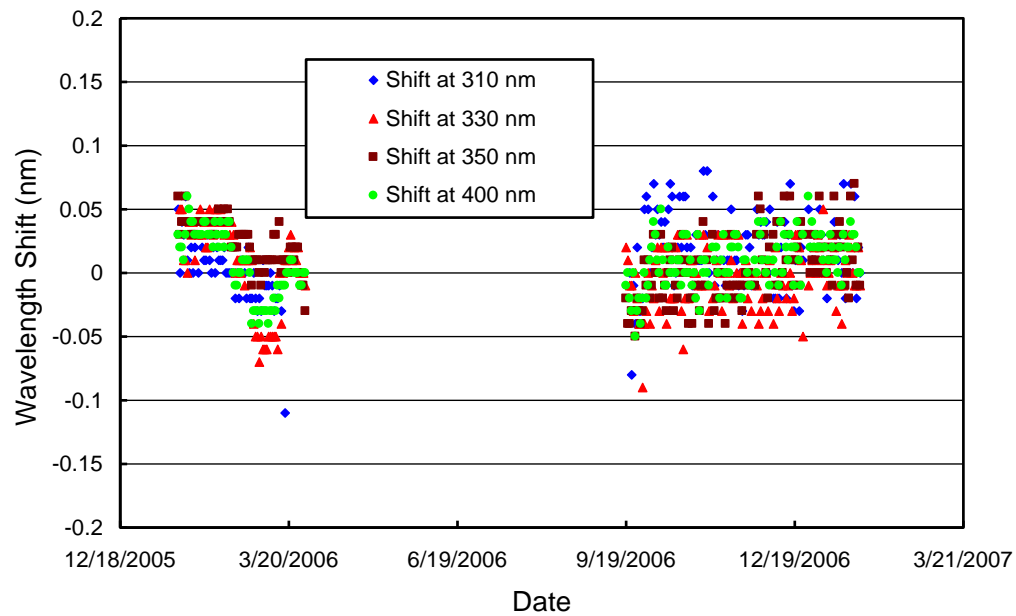


**Figure 5.3.9.** Wavelength accuracy check of final data at four wavelengths by means of Fraunhofer correlation. Measurement performed at 00:00 UT were evaluated for each day of the season. No data exist during Polar Night.

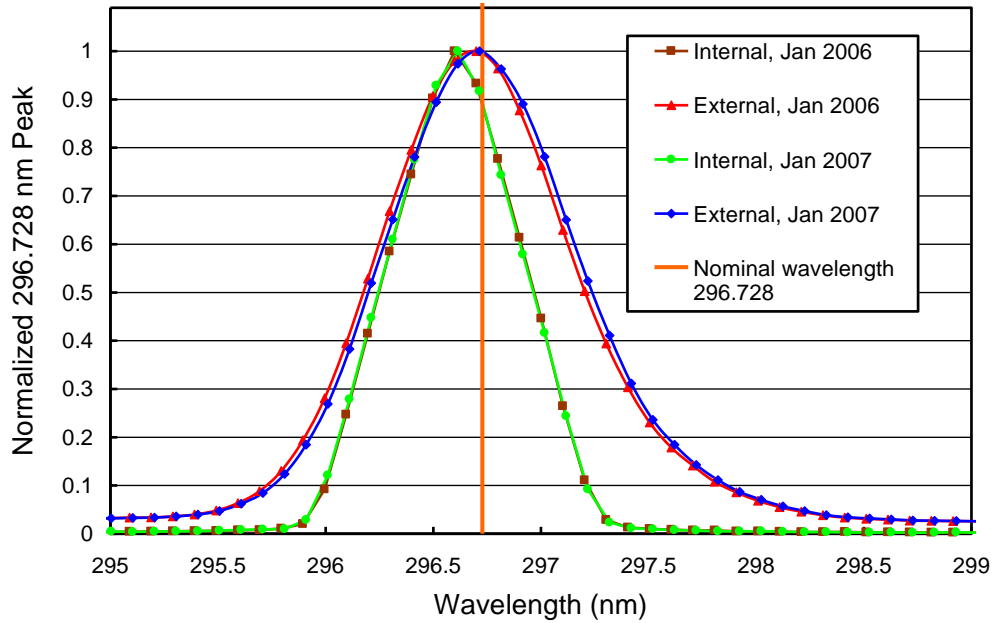


Figure 5.3.10. The 296.73 mercury line as registered by the PMT from external and internal sources.

**5.3.4. Missing Data**

A total of 17690 scans are part of the published South Pole Volume 16 dataset. These are about 91% of the maximum possible number of data scans. 916 solar scans were superseded by calibration scans. Since South Pole Station has 24 hours of sunlight per day during the summer season, a loss of solar data cannot be avoided. About 4% of all possible scans were missed due to technical problems including station-wide power outages. A break-down of missing data is provided in Table 5.3.2

**Table 5.3.2. Missing solar scans in the South Pole Volume 16 data set.**

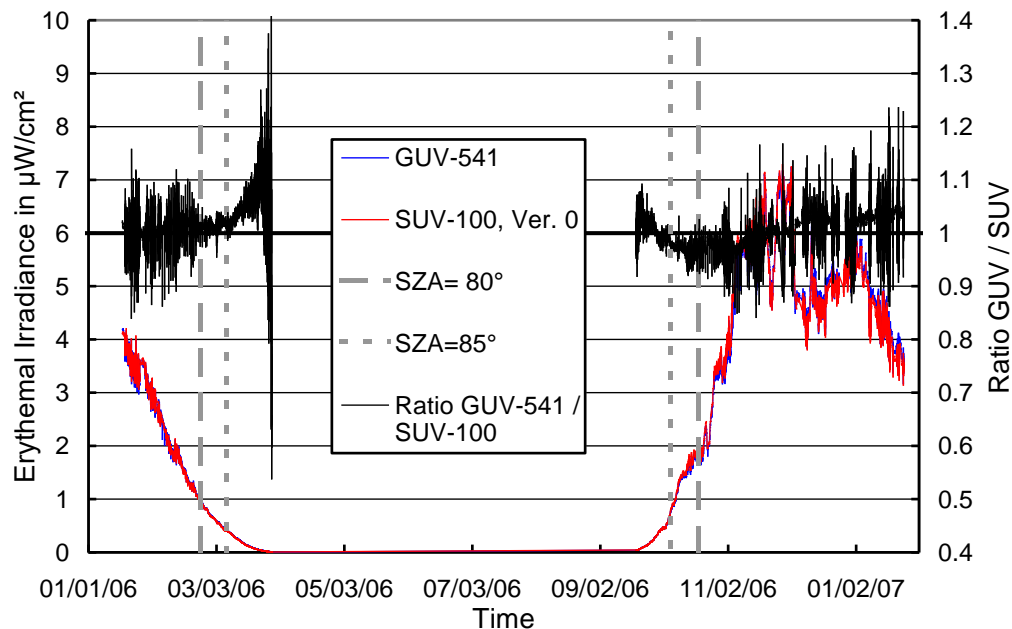
Period	Number of scans	Reason
<i>Calibration scans</i>		
Throughout season	369	Response scans
Throughout season	435	Wavelength scans
Throughout season	112	Absolute scans
<i>Technical problems</i>		
01/18/06	20	Missing for unknown reasons
02/27/06	2	Investigation of errors generated by wavelength sensor
09/15/06 – 09/18/06	353	Software “hung”
11/26/06 – 11/27/06	133	Power outage not buffered by UPS
12/2/06	14	Monochromator interface (“Spectralink”) unresponsive
12/06/06 – 12/07/06	100	Power outage not buffered by UPS
12/25/06 – 12/26/06	117	Power outage not buffered by UPS
12/29/06	44	Power outage not buffered by UPS
<i>Other</i>		
Throughout season	27	Collector shaded by nearby obstacles, e.g. air sampling stack

### 5.3.5. GUV Data

The GUV-541 radiometer, which is installed next to the SUV-100, was calibrated against final SUV-100 measurements following the procedure outlined in Section 4.3.1. The calibration of the instrument's 320 nm channel drifted by 6.5% over the course of the year. Drifts of other channels were smaller than 3%. To corrected for these changes, data recorded before and after the period of winter darkness were processed separately, and different calibration factors were applied for the two periods. Drifts in published GUV data are smaller than 3%.

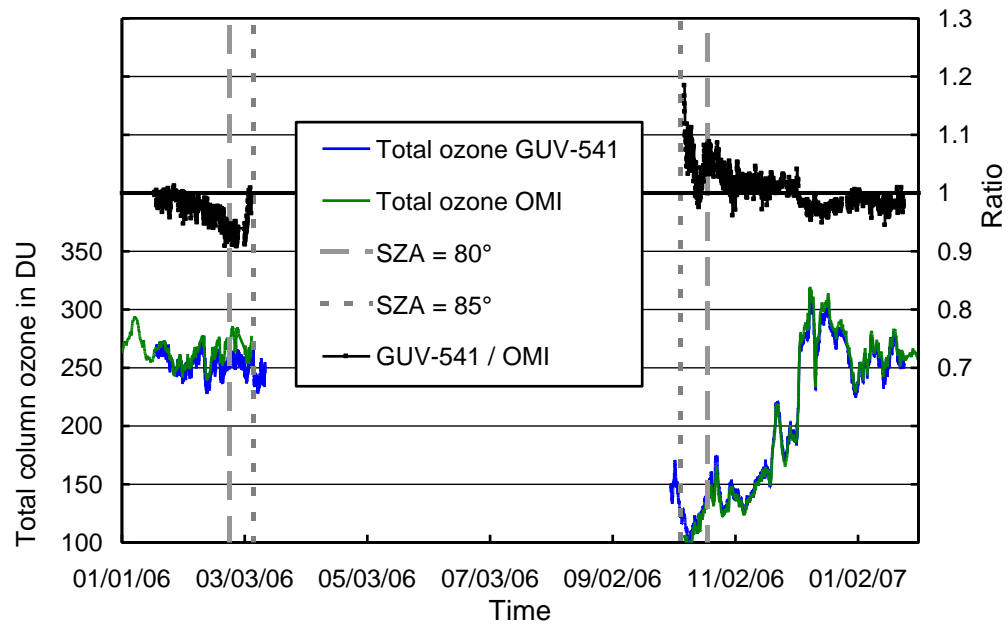
From the calibrated measurements, data products were calculated (Section 4.3.2). Figure 5.3.11. shows a comparison of GUV-541 and SUV-100 erythemal irradiance based on final Volume 16 data. For solar zenith angles smaller than  $80^\circ$ , measurements of the two instruments agree to within  $\pm 3\%$  ( $\pm 1\sigma$ ), except for times when an air sampling stack installed at the ARO building casts a shadow on the GUV-541 radiometer but not on the SUV-100.<sup>+</sup> We advise data users to use SUV-100 rather than GUV-541 data whenever possible, in particular for low-Sun conditions.

Figure 5.3.12 shows a comparison of total ozone measurements from the GUV-541 radiometer and the Ozone Monitoring Instrument (OMI) installed on NASA's AURA satellite. GUV-541 ozone values were calculated as described in Section 4.3.3. In the austral spring, the two datasets agree well for SZAs smaller than  $80^\circ$ . There is a bias of about 5% for the second half of February 2006. A similar bias is also observed in previous years. The reason of this bias is still unresolved, but could be caused by the choice of the ozone profile used in the calculation. For SZA larger than  $80^\circ$ , GUV-541 data become unreliable and should not be used.



**Figure 5.3.11.** Comparison of erythemal irradiance measured by the SUV-100 spectroradiometer and the GUV-541 radiometer. SUV-100 measurements are based on “Version 0” (cosine-error uncorrected) data.

<sup>+</sup> SUV-100 data affected by shading from the air sampling stack have been excluded from the published data set. GUV-541 data concurrent with shaded SUV-100 measurements have also been excluded. Since the SUV-100 collector is located approximately 2 meters away from the GUV-541 radiometer, both instruments are not shaded during exactly the same time and some data affected by the stack are still part of the GUV-541 data set.



**Figure 5.3.12.** Comparison of total column ozone measurements from GUV-541 and OMI. GUV-541 measurements are plotted in 15 minute intervals. For calculating the ratio of both data sets, only GUV-541 measurements concurrent with OMI overpass data were evaluated.